Electronic structure of the LaS surface and LaS/CdS interface

O. Eriksson
Theoretical Division and Center for Materials Science, Los Alamos National Laboratory, Los Alamos, New Mexico 87545 and Department of Physics, Uppsala University, Box 530, Uppsala, Sweden

John Wills
Theoretical Division, Los Alamos National Laboratory, Los Alamos, New Mexico 87545

P. Mumford
Wright Laboratory, Wright-Patterson Air force Base, Dayton, Ohio 45433

M. Cahay
Department of Electrical and Computer Engineering and Computer Science, University of Cincinnati, Cincinnati, Ohio 45221

W. Friz
Multi Area Research in Science (MARS) Consultants, Fairborn, Ohio 45324
(Received 12 September 1997)

The electronic structure of the LaS surface and CdS/LaS interface is calculated by means of a first-principles electronic-structure method for slab and bulk geometries. The calculations were based on the local-density approximation to density-functional theory and made use of linear muffin-tin orbitals as basis functions for solving the Kohn-Sham equations. The observed low work function of LaS is reproduced by our theory and the calculated surface relaxation of LaS is found to be very small. It is further found that NaCl structured layers of LaS should grow in a well-behaved, epitaxial way on a CdS substrate with a ZnS structure. The interlayer spacing between the first atomic layer of LaS and the topmost layer of the CdS substrate is found to be close to the interlayer distances in both LaS and CdS. The LaS/CdS geometry should thus be possible to grow, and may be a good candidate for cold electron emitter devices. [S0163-1829(98)07007-6]

I. INTRODUCTION

Recently, there has been renewed interest in cold cathode emitters for applications to a variety of electronic devices, including microwave vacuum transistors and tubes, pressure sensors, thin panel displays, high temperature and radiation tolerant sensors, among others.[1–4] The technical possibility of a uniformly emitting surface cathode that operates at room temperature appears to be an attractive prospect; in particular, if such an emitter could yield electron current densities comparable to or better than existing thermionic technology available today. For microwave tube applications, achieving an emission current density in excess of 10 A/cm^2 with an associated emission lifetime of at least 10^5 h is our goal. Low-temperature operation in nonthermionic electron emitters is very desirable for keeping the statistical energy distribution of emitted electrons as narrow as possible, to minimize thermal drift of solid state device characteristics, and to avoid accelerated thermal aging or destruction by internal mechanical stress and fatigue. Minimizing the temperature rise of the emitter appears quite possible if they are constructed as thin epitaxial films using vertical layering technology due to the extremely short heat paths and excellent heat-sinking possibilities offered by this architecture.

Use of a thin film of LaS grown latticed matched to an underlying film of CdS has been suggested as a structure suitable for producing a cold cathode electron emission device.[4–7] In this cathode, a high injection efficiency of electrons into vacuum relies on Fowler-Nordheim injection of electrons at a metal (or n^{++}-InP; indium phosphide)/CdS(cadmium sulfide) interface, ballistic transport through the CdS layer, and negative electron affinity (NEA) at the CdS surface coated with a semimetallic thin film of LaS (lanthanum sulfide). The NEA concept implies that, because of the low work function of the LaS thin film,[8] the vacuum level outside the cathode is located energetically below the conduction-band edge of the wide-band-gap semiconductor (CdS). Based on these assumptions, it was shown[5–7] that under forward bias operation electrons captured in the LaS thin film cause an effective reduction of the work function of the semimetallic thin film. As a consequence a substantial increase of the cold cathode emitted current was found. It was shown[5] that the new cold cathode emitter is capable of achieving low-voltage (<10 V) room-temperature operation with an emission current density approaching 100 A/cm^2.

The development of innovative electron emitter materials, structures, and devices is needed to support evolving vacuum electronic technologies to satisfy future requirements for microwave tube sources such as greater compactness, robustness, and wider operating frequency range. Advanced emitter devices that support the spatial and temporal modulation of a high current density electron source attack these requirements directly. Use of materials engineering to tailor the internal electronic structure of a device along with advanced microfabrication capabilities to define precise geometric features enables the controlled injection, transport, and emission

of electrons in a cold cathode emitter. In this paper we investigate the electronic structure of LaS and, specifically, of a thin film of LaS on CdS. On top of having the required electronic properties the different layers in the proposed cold cathode have quite similar lattice constants, which is required for good epitaxial growth and device production. The choice of InP as a substrate is particularly attractive since the lattice constant of InP (5.86 Å) closely matches the lattice constant of the zinc-blende cubic CdS (5.83 Å). Furthermore, LaS in its cubic phase has a lattice constant equal to 5.85 Å and is therefore nearly lattice matched with CdS.

Although a good lattice match is required to promote good growth conditions at the substrate surface, it does not ensure growth of a single-crystal film. Before embarking on the relatively expensive experimental task of epitaxial growth, it is important to use less costly theoretical modeling methods to guide the investigation. This modeling provides an estimate of such qualities as surface layer relaxation, interface relaxation, and whether the interface will be energetically stable or not. This paper addresses these issues by means of total-energy calculations based on the local-density approximation to density-functional theory. We have thus calculated bond lengths between atoms at the interface and obtained the energy at the interface. In addition, we have calculated the atomic displacements on the LaS surface layer, i.e., the surface layer relaxation.

Previous work on LaS dealing with the electronic structure involve point contact spectroscopy,[9] measurements of the reflectivity,[10] and calculations of the electronic structure,[11] dielectric constants,[12] and x-ray absorption.[12] In addition the phonon spectrum was calculated by Steiner, Eshrig, and Monnier.[13]

II. DETAILS OF THE CALCULATIONS

The calculational method used in the present work is a so-called full-potential linear muffin-tin orbital (LMTO) method, for bulk[14] and slab geometries,[15] which is based on the local-density approximation[16] (LSDA) to density-functional theory. In the bulk calculations we adopt a base geometry consisting of muffin-tin spheres and an interstitial region, whereas for the slab calculations we also introduce a surface region. The interstitial basis function is a Bloch sum of Neuman and Hankel functions. Each Neuman or Hankel function is then augmented (replaced) by a numerical basis function inside the muffin-tin spheres, in the standard way of the linear muffin-tin orbital method.[17] In the slab method the Neuman and Hankel functions are replaced by numerical functions also in the vacuum region.

The present calculations are all-electron as well as scalar relativistic. The latter is achieved by including the mass velocity and Darwin terms (and higher-order terms) in the calculation of the radial functions, inside the muffin-tin spheres, whereas the spin-orbit coupling was omitted. Moreover, the present calculations made use of a so-called double basis, to ensure a well converged basis set. This means that we used two Hankel or Neuman functions each attaching to its own radial function for each set of (n,l) quantum number. We thus had a set of two $5s$, $5p$, $6s$, $6p$, $5d$ and $4f$ basis functions centered on the La atom and two $3s$, $3p$, and $3d$ basis functions centered on the S atom and two $5s$, $5p$, and $4d$ basis functions on the Cd atom.

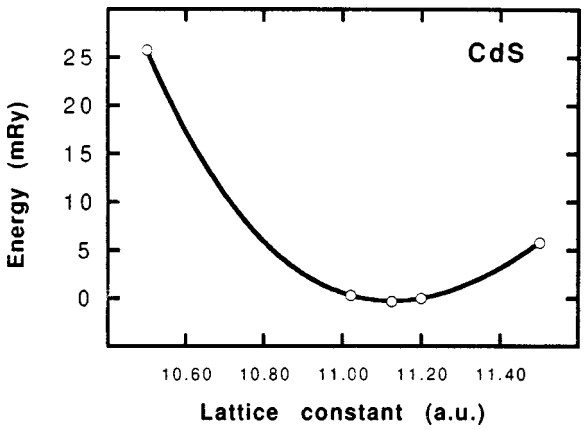

FIG. 1. Calculated total energy of bulk CdS as a function of lattice constant.

The slab calculations were made with 7 LaS atomic layers, to ensure bulk behavior for the central layer and the CdS/LaS calculations were made with 5 CdS layers sandwiched between 3 LaS layers on each side. In this way both the interface electronic structure and geometry is obtained in parallel to information about the surface electronic structure and geometry of the CdS/LaS system.

III. RESULTS

A. Results for bulk LaS and CdS

As a precursor to the surface and interface calculations we performed a geometry optimization of bulk CdS, shown in Fig. 1. The resulting theoretical equilibrium lattice constant is at 11.12 a.u., which should be compared to the experimental one of 11.01 a.u. In Fig. 2 we show the density of states of CdS. CdS comes out to be a semiconductor in our calculation—in agreement with experiment. The size of the band gap is calculated to be $\sim$ 1.1 eV and is substantially

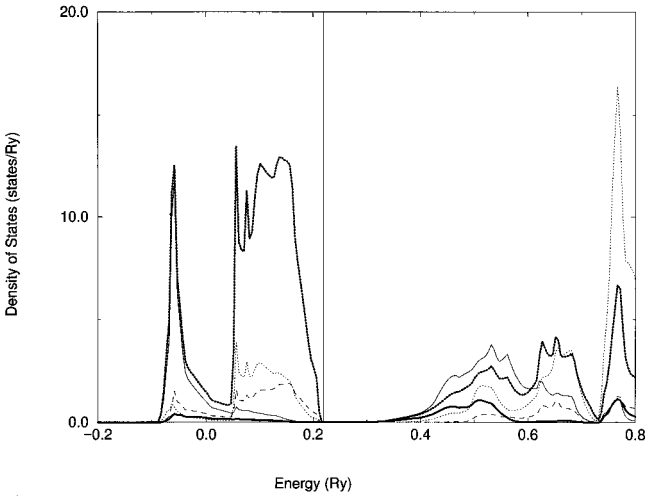

FIG. 2. Calculated density of states (DOS) for bulk CdS. The Cd states are shown with thin lines and the S states with thick lines. The *s* projected DOS is shown with full lines, the *p* projected DOS with dotted lines and the *d* projected DOS with dashed lines. Energy is in Rydbergs and the Fermi level is shown as a vertical line.

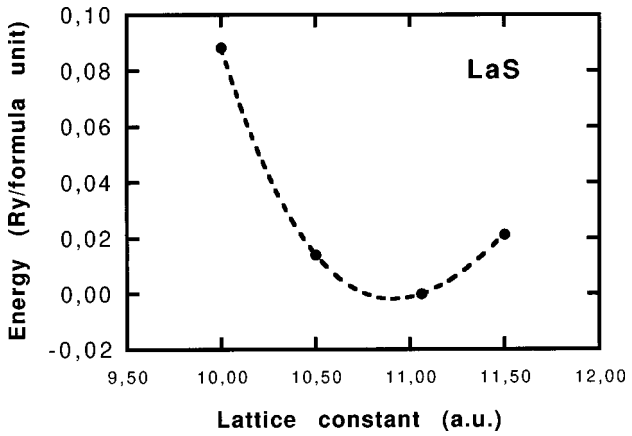

FIG. 3. Calculated total energy of bulk LaS as a function of lattice constant.

smaller than the experimental value ($\sim$ 2.5 eV). In these types of calculations the size of the band gap typically does not agree very well with experiments, a well-known problem with LDA calculations. However, the presence or absence of a gap should be in agreement with observations and in this case it is. Notice in Fig. 2 that the occupied part of the density of states (DOS) is dominated by Cd s and S p orbitals, which hybridize and intermix strongly. In addition there is a rather large Cd p and Cd d component to the occupied part of the DOS.

Next we performed a geometry optimization of cubic LaS (Fig. 3). The theoretical lattice constant is 10.91 a.u. and is in agreement with an experimental value of 11.06 a.u. The DOS of bulk LaS is shown in Fig. 4. Notice that we are only showing the dominating partial DOS, i.e., S $3p$, La $5d$, and La $4f$. The occupied part of the DOS is dominated by the S p and La d states, whereas the La f states form a conspicous peak at $\sim$ 1.5 eV above the Fermi level (E_F). The importance of the $4f$ states for the dynamical work-function shift will be discussed below. In Fig. 5 the energy band dispersion corresponding to the DOS in Fig. 4 is displayed.

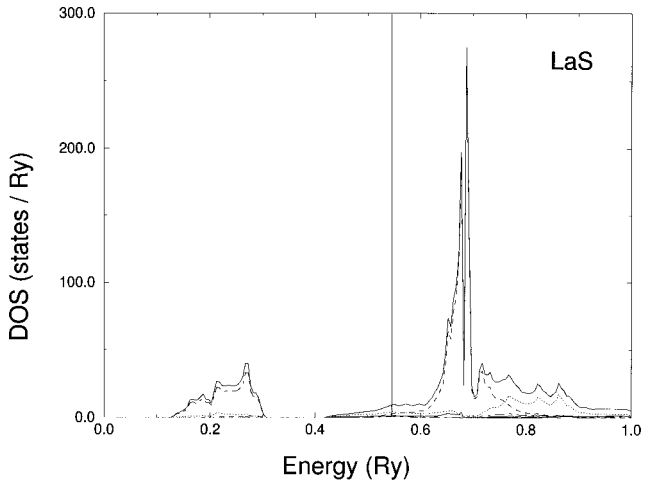

FIG. 4. Calculated density of states for bulk LaS. The total DOS is shown as a full line, the S p projected DOS is given as a dashed-dotted line, the La d projected DOS is shown as dotted lines, and the La f DOS is shown as a dashed line. Energy is in Rydbergs and the Fermi level is shown as a vertical line.

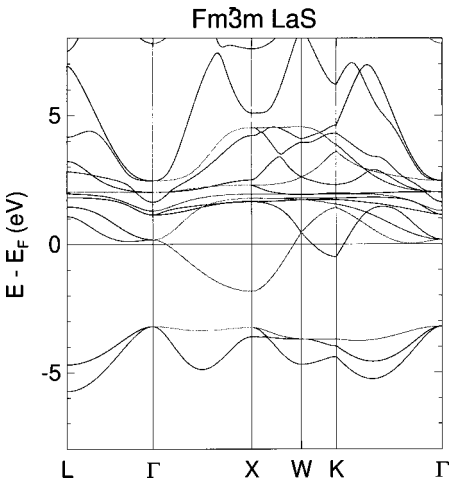

FIG. 5. Calculated energy bands of LaS along different high symmetry directions in the Brillouin zone. Energy is in electron-volts and the Fermi level is shown as a horizontal line.

In practical applications it is envisioned that a few layers of LaS should coat a CdS substrate.[5] Since the small lattice mismatch between CdS and LaS is expected to introduce a small tetragonal shear in LaS we calculated, as a precursor to the surface calculations, the tetragonal shear of bulk LaS, keeping the lattice constant in the ab plane fixed to the observed CdS bulk lattice constant. We thus calculated the total energy of tetragonal LaS as a function of the c/a ratio, keeping the in-plane lattice constant equal to 11.01 a.u. (Fig. 6). As seen in the figure, the LaS c-lattice constant is decreasing only with a small amount from a theoretical bulk value of 10.90 a.u. to a value of 10.80 a.u. The important thing to note here is that there is only a small change in the c-lattice constant associated with constraining the LaS in-plane lattice constant to the value of bulk CdS.

B. The surface of LaS

In Fig. 7 we show the calculated total energy of the LaS surface as a function of the relaxation in the 001 direction of the topmost atomic layer. All atomic planes in this surface calculation had in-plane lattice constants equal to the value of bulk CdS. The lower-lying atomic planes had a fixed c-lattice constant of 10.80 a.u., i.e., a value equal to the

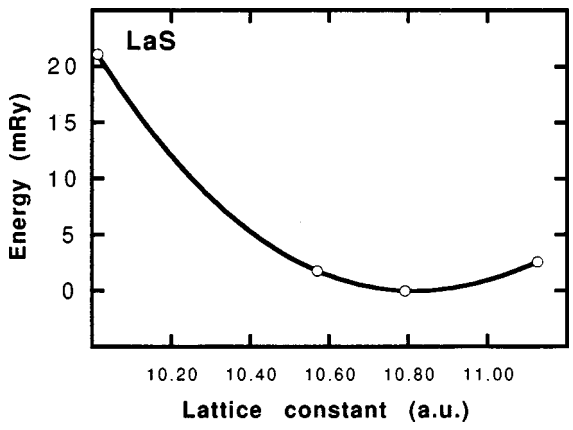

FIG. 6. Calculated total energy of tetragonal bulk LaS as a function of c lattice constant.

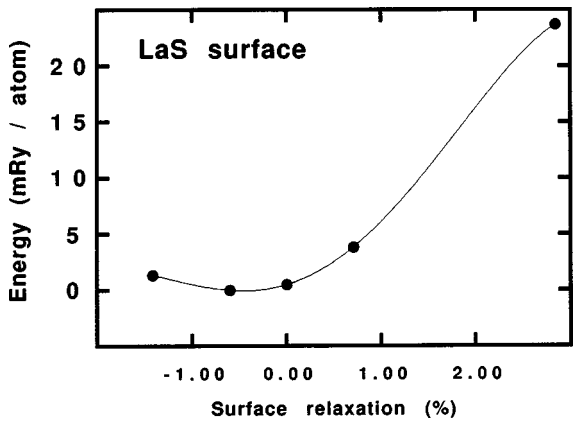

FIG. 7. Calculated total energy of a seven-layer LaS slab as a function of the surface relaxation.

calculated value of Fig. 6. From the figure it becomes clear that the surface atoms undergo only a small inwards relaxation of $\sim$ 0.5 %. Also, the energy change associated with the surface relaxation is quite small, of the order of a fraction of a milliRydberg when comparing the relaxed and unrelaxed configurations. Such a small number is roughly the same as the accuracy of first-principles calculations of surface relaxations.

The density of states (DOS) of the geometry-optimized LaS surface is shown in Fig. 8. In this figure we compare the DOS of the surface and center layer La atoms, since most of the modifications in the electronic structure at the surface come from basis states centered on the La atoms. For instance, at the surface the La f DOS is substantially more narrow than the bulk projected La f DOS. This is caused by the reduced number of nearest neighboring atoms at the surface. Despite the modification of the electronic structure at the surface, the surface of LaS remains a conductor since the DOS is nonzero at energies greater than the Fermi energy. Also, for the d orbitals the narrowing at the surface is less dramatic as seen in Fig. 8. These orbitals are more extended in space and are hence less influenced by the reduced number of nearest neighbors. The S projected DOS of all atomic layers in the slab is quite similar to the bulk DOS given in Fig. 4, and for that reason are not shown.

We also analyzed the charge-density contour of the LaS surface (figure not shown) and it revealed no or few signs of covalent bonding (which would have charge piling up between atoms). There is no pronounced charge transfer between the different atoms and hence the bonding in LaS is best characterized as metallic. At the surface there is an increased tendency of a non-spherical density, which is typical for surface geometries when charge is spilling out in the vacuum.

The calculated work function for the LaS surface is $\sim$ 0.9 eV and agrees rather well with the observed value of $\sim$ 1.1 eV.[5–7]

C. The LaS/CdS interface

In this section we describe the results for the CdS/LaS interface surface. We first optimized the interplanar distance between the CdS and LaS layers in a slab calculation involving 5 CdS layers (with a ZnS structure) sandwiched between

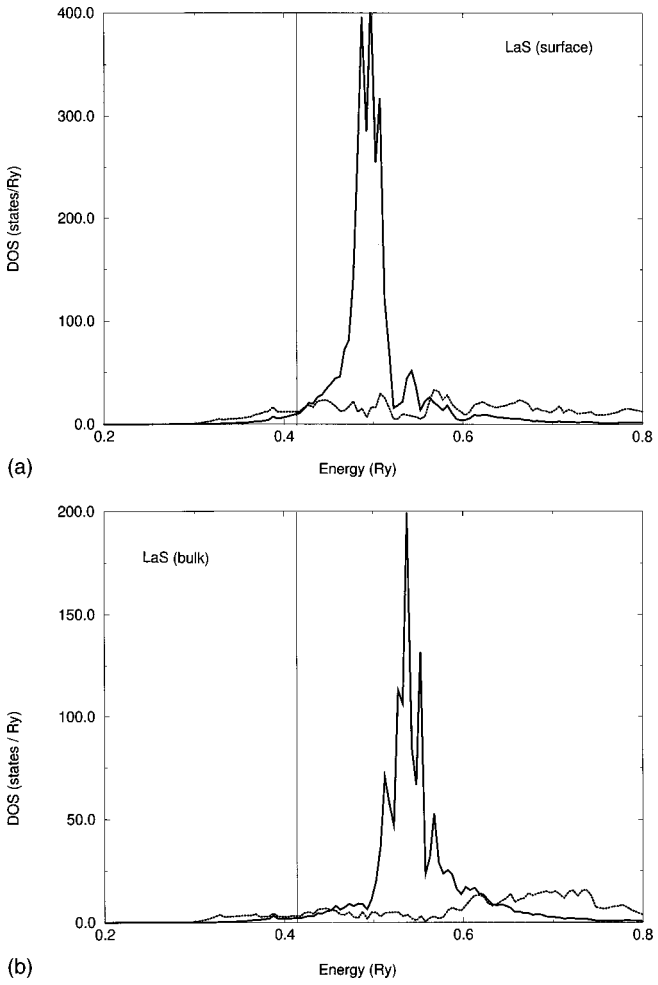

FIG. 8. Calculated density of states for a seven layer slab of LaS. Only the d- (dotted lines) and f-projected (full lines) DOS of the surface (a) and center (b) La atom are given. Energy is in Rydbergs and the Fermi level is shown as a vertical line.

3 (rock salt structured) LaS layers on each side. The interplanar distance is calculated to be 5.41 a.u. (Fig. 9), to be compared to the experimental interplanar distance in LaS, which is 5.53 a.u. and the observed distance between different atomic layers of Cd in CdS, which is 5.51 a.u. This

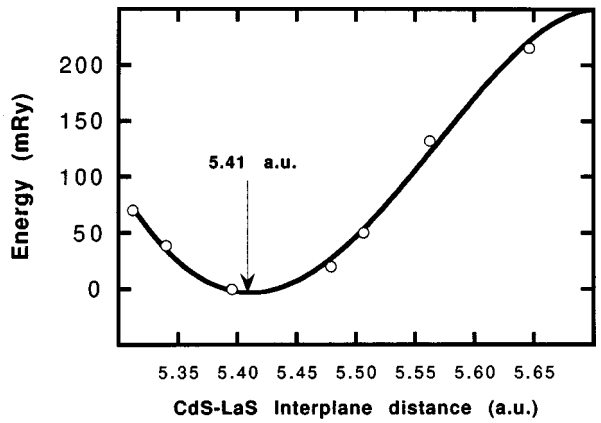

FIG. 9. Calculated total energy of a CdS/LaS slab as a function of the CdS-LaS interface distance.

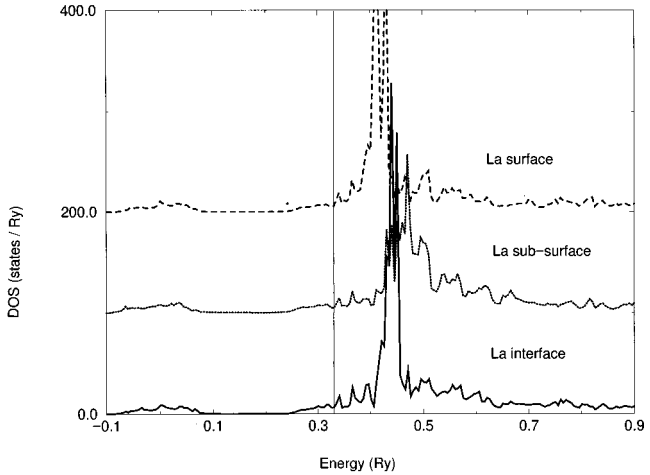

FIG. 10. Calculated density of states for a slab of CdS/LaS. Only the DOS projected on the La atoms at the surface (solid line), subsurface (dotted line), and interface (dashed line) are given. Energy is in Rydbergs and the Fermi level is shown as a vertical line.

calculation was performed keeping the in-plane lattice constant equal to the value of bulk CdS. We should thus compare the value 5.41 a.u. with the interplanar atomic distance of the ''tetragonal optimized'' value of bulk LaS with an ab lattice constant kept equal to the bulk CdS value. In this geometry the interplanar distance was 5.40 a.u. (Fig. 6). There is thus not a big influence of the CdS substrate on the interatomic distances of the LaS overlayer. The surface relaxation of LaS, when put on top of CdS, is the same (within the accuracy of our calculations) as the relaxation of the pure LaS surface calculation, i.e., a $\sim$0.5% inwards relaxation (as shown in Fig. 7).

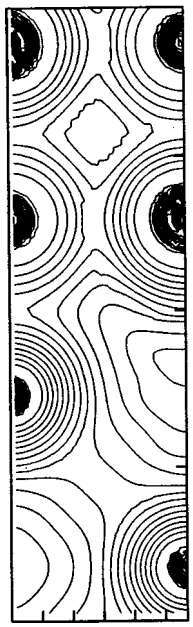

FIG. 11. Charge density contour of CdS/LaS for a section focused on the interface. The Cd atoms are the lowermost two atoms. In this figure there is a La atom in the top left corner of the figure. Below this La atom there is a S atom. There is also a S atom in the upper right corner of this figure that has a La atom just below it.

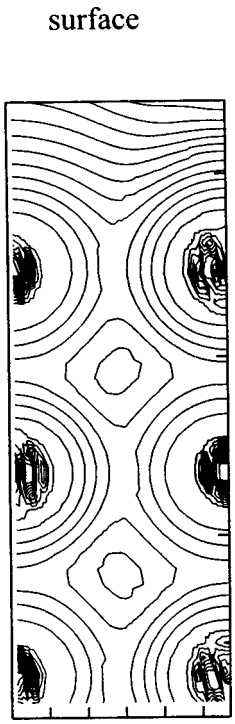

FIG. 12. Charge density contour of CdS/LaS for a section focused on the surface. The surface is at the top in the figure. The atoms to the left are stacked as S, La, S when going from the deeper layers to the surface. On the right hand side in the figure the stacking is La, S, La.

In Fig. 10 we display the DOS curves for the La projected states of the LaS/CdS slab. We show only the DOS projected on La, since most of the modifications due to the surface/interface geometry are found for these states. As seen in this figure the La f DOS is narrower at the surface and interface compared to the La atoms deeper in the overlayer. This is due to a reduced number of, primarily, neighboring S atoms. The S p states (not shown) are found to be very similar for the surface and subsurface, and the bandwidth is about the same for the two atomic positions. Although CdS is a semiconductor with zero DOS at the Fermi level, the interaction with the LaS overlayer causes the Cd and S interface projected DOS to be metallic. Thus, even though atomistically there is a sharp boundary between the LaS and CdS layers, the transition is electronically smoother, where the transition from metallic behavior in the LaS to semiconducting behavior in CdS takes place over a few atomic CdS layers. The deeper atomic layers of CdS are similar to bulk CdS, being semiconducting with a zero DOS at the Fermi level.

We end this section by showing in Figs. 11 and 12 the charge density contour of the CdS/LaS 001 overlayer for a cut in the 010 direction. The surface direction (001) is pointing upwards in the figures. In Fig. 11 we show the charge-density contour in the vicinity of the interface and in Fig. 12 we show the charge-density contour of the surface atoms. As regards the surface (Fig. 12) there are aspherical features in the vicinity of the vacuum region, whereas otherwise the density contour is rather spherical. As seen in Fig. 11 the

charge density is essentially symmetric around all atoms in the metallic layer whereas in the semiconducting region the density contour is more typical of a covalently bonded system. This suggests that from a chemical bonding view the transition from the metallic region to the semiconducting region is sharp, in contrast to the transition in the electronic properties which as discussed in connection to Fig. 10 is smoother. Also, in the CdS/LaS interface/surface calculation there is very little charge transfer at the interface, suggesting that there is only a minor ionic component to the chemical bond.

IV. DISCUSSION AND CONCLUSION

The total-energy calculations presented here show that it is quite possible to grow overlayers of LaS (with a rock-salt structure) on a CdS substrate (with ZnS structure). There will only be a small amount of surface relaxation and only a small relaxation of the inter-plane distances at the interface. This is useful knowledge when trying to grow materials for use as cold electron emitter devices. Also, in practical applications the device, which is modeled here, is designed to be used in forward bias, and as a consequence electrons are captured in the LaS quantum well.[5] This means that electrons will occupy LaS states that in Fig. 8 are above the Fermi level. The narrow $4f$ band at $\sim$ 1.5 eV above E_F is likely to be important for capturing electrons in the semimetallic overlayer, since the electron mobility of these states is very low, which in turn is important for the dynamical work-function shift.[5] A theoretical treatment of f electrons is sometimes hard. Fortunately this is less of a problem for La and La-based compounds, where it is known that the f levels form a rather wide band, which is situated above E_F. In certain cases an unoccupied f level may be detected by electron spectroscopy and good agreement between first-principles theory is observed, as demonstrated by, for instance, Weschke *et al.*[18] The position and width of the presently calculated f-level should thus be rather accurate.

In addition we find that the electronic structure of the LaS overlayer on CdS is quite similar to the electronic structure of a LaS surface. The transition from metallic to semiconducting behavior at the interface is found to be smooth electronically, since the first layers of CdS are metallic. This contrasts to the chemical bonding where the transition in the overlayer should be sharp, from metallic to covalentlike bonding. Finally, the observed low work function of LaS is reproduced.

ACKNOWLEDGMENTS

O.E. wishes to acknowledge support from the Swedish Materials Consortium No. 9. Valuable help from Dr. M. Steiner is acknowledged.

[1] I. Brodie and C.A. Spindt, *Vacuum Microelectronics* (Academic Press, New York, 1992).

[2] I. Brodie and C. A. Spindt (unpublished).

[3] S. Ianazzo, Solid State Electron. **36**, 301 (1993).

[4] The work presented here follows suggestions that are documented in two in-house reports by W. Friz, Wright-Patterson Air Force Base Final Technical Report, Task ELM-9, June 1992, and Wright-Patterson Air Force Base Technical Note, Task ELM-6, January 1995.

[5] P. D. Mumford and M. M. Cahay, J. Appl. Phys. **79**, 2176 (1996).

[6] P. D. Mumford and M. M. Cahay, J. Appl. Phys. **81**, 3707 (1977).

[7] P. D. Mumford and M. M. Cahay, in *Proceedings of the 26th Conference on the State-Of-The-Art Program on Compound Semiconductors* (The Electrochemical Society, Montreal, 1997), Vol. 97-1, p. 242.

[8] The room temperature work function for LaS is estimated to be 1.14 eV by extrapolating measured work function values at high temperature as reported by S. Fomenko, in *Handbook of Thermionic Properties* (Plenum, New York, 1966). Within the range of temperature investigated by Fomenko, the LaS work function increases with temperature at a rate of 2 meV/K.

[9] I. Frankowski and P. Wachter, Solid State Commun. **40**, 885 (1981).

[10] W. Beckenbauch, J. Evers, G. Günterhof, E. Kaldis, and P. Wachter, J. Phys. Chem. Solids **36**, 239 (1975).

[11] Z. W. Lu, D. J. Singh, and H. Krakauer, Phys. Rev. B **37**, 10 045 (1988).

[12] S. V. Vlasov and O. V. Ferberovich, Solid State Commun. **56**, 967 (1985).

[13] M. M. Steiner, H. Eschrig, and R. Monnier, Phys. Rev. B **45**, 7183 (1992).

[14] J. M. Wills (unpublished); J. M. Wills and B. R. Cooper, Phys. Rev. B **36**, 3809 (1987); D. L. Price and B. R. Cooper, *ibid.* **39**, 4945 (1989).

[15] J. M. Wills and O. Eriksson (unpublished).

[16] U. von Barth and L. Hedin, J. Phys. C **5**, 2064 (1972).

[17] O. K. Andersen, Phys. Rev. B **12**, 3060 (1975); H. L. Skriver, *The LMTO Method* (Springer, Berlin, 1984).

[18] E. Weschke, C. Laubschat, R. Ecker, A. Höhr, M. Domke, G. Kaindl, L. Severin, and B. Johansson, Phys. Rev. Lett. **69**, 1792 (1992).